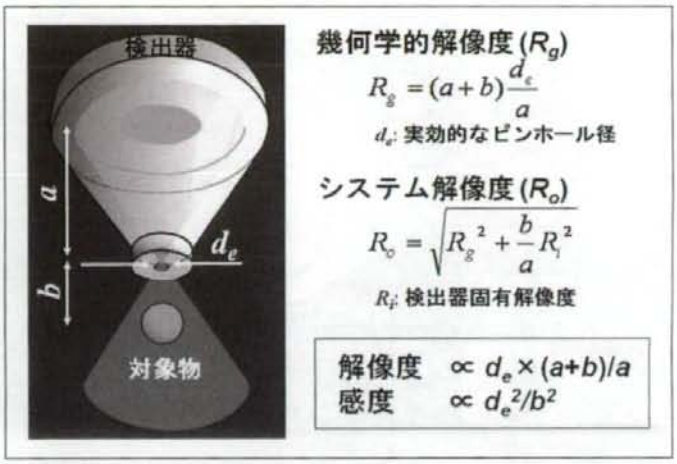

図1　ピンホールSPECTによる拡大撮像
撮像対象をコリメータに近づけるほど解像度や感度が改善される。

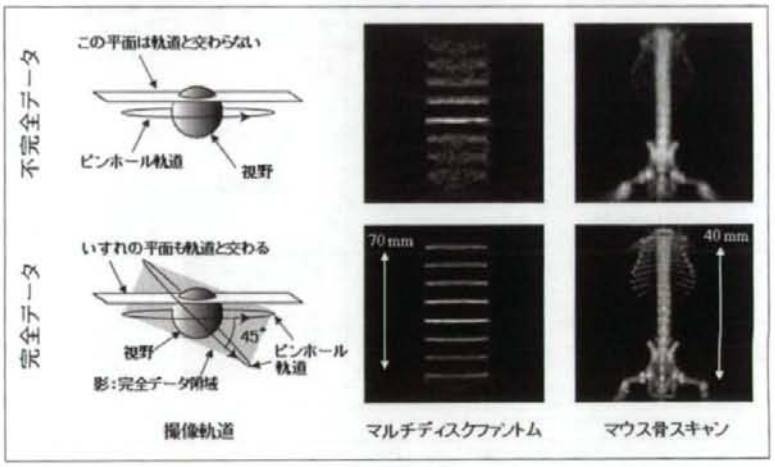

図2　従来の単一円軌道からの不完全データ（上）と開発した2軸収集軌道からの完全データ（下）による再構成画像の比較
マルチディスクファントム実験とマウス骨スキャン。従来法では画像中央断面以外は大きく歪み、完全データから再構成した画像では歪がなく、視野全体で均一な解像度が得られている。0.5mmの肋骨も鮮明に描出されている。

これに対応した3次元OSEM画像再構成法を開発した[5]。これによって、歪みのない視野全体で均一な解像度を有する3次元画像を得ることに成功した。その結果、ピンホールSPECTにおいても定量評価が可能になった。同様の試みとして、Metzlerらはヘリカル軌道によって完全データ収集し、画像歪を改善することを示した[6]。また、Beekmanらは多数のピンホールで被写体を囲むことで、検出器を静止した状態で近似的な完全データを得ている[7]。

トランケーションを許す画像再構成法

ピンホールコリメータは、撮像対象がコリメータに近いほど感度および解像度を高くできるのが特長であるが、極端に近づけるとトランケーションが生じる。その結果、再構成画像の視野の周辺で極端にカウントが高くなるアーチファクトが生じ、画像全域でもカウントが過大評価されるので、定量評価の妨げとなる。

小動物を撮像する場合は、通常、被写体が視野からはずれないように、被写体からコリメータをある程度遠ざけて撮像する。ただし、これは解像度と感度について妥協することになる。われわれは、Defriseらが2次元X線CTを対象として提案したトランケーションを許す画像再構成理論[8]を基に、これをピンホールSPECTに拡張した3次元画像再構成法TC-

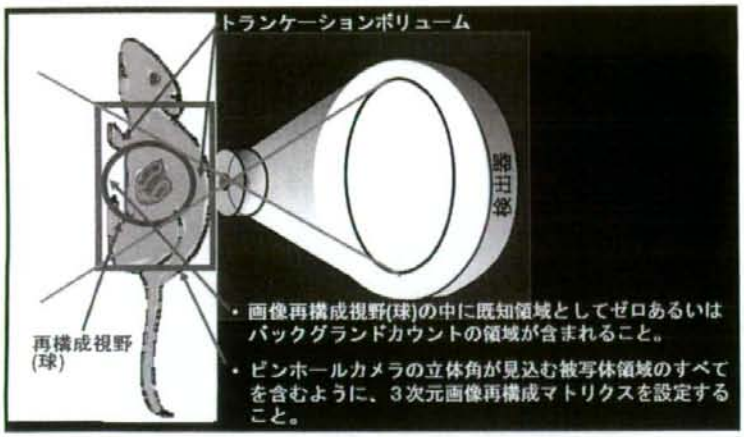

図3　ピンホールSPECTの3次元画像再構成において、トランケーションがあっても視野内は正確な画像を得るための再構成条件

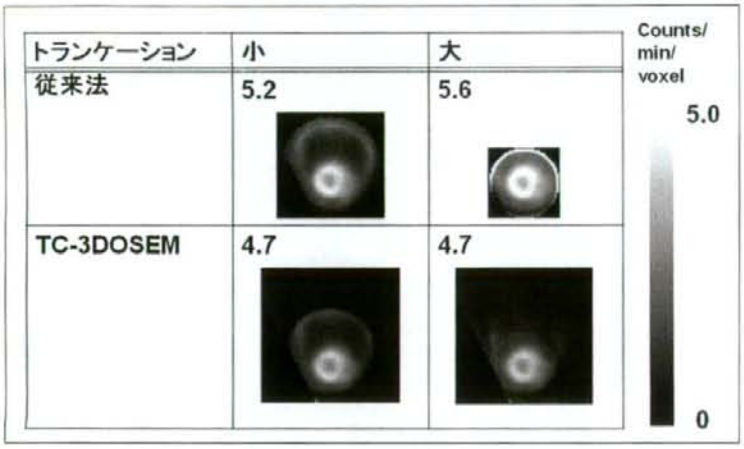

図4　TC-3DOSEMと従来法によって再構成されたラット心筋画像と心筋カウント

数値は心筋上のROIの平均カウント。実験データからトランケーション量の異なるデータを生成した。TC-3DOSEMではアーチファクトおよび過大評価が抑制され、またトランケーション量に依存しない定量画像が得られる。

3DOSEM（Truncation Compensated 3DOSEM）を開発した[9]。本画像再構成理論では、**図3**に示すように、①画像再構成視野（球）の中に既知領域として被写体の外側のゼロあるいはバックグランドカウントのボリュームが含まれること、および②ピンホールカメラの立体角が見込む被写体領域をすべて含むように3次元画像再構成マトリクスを設定すること、この2つの条件下において、OSEMなどの逐次近似画像再構成法によって視野内は正確な値に収束する。本手法によって、トランケーションがあっても視野内においては定量性が確保される（**図4**）。

小動物用SPECT装置

われわれは、ラットの心筋血流量定量などを目的とした、小型で可搬性のある小動物専用SPECT装置を開発した。装置を小型化するために導入した小型高解像度検出器は、シンチレータが臨床用SPECT装置で使用されているような平板のNaIに代えて1.5mmピッチのピクセル型NaIを使用し、光電子増倍管（Photomultiplier Tube: PMT）も、従来の3インチの大型PMTによる配列に代えて5cmのフラット位置感応型PMTで構成されている。小型高解像度検出器とピンホールコリメータの拡大撮像技術を組み合わせ[10]、コ

図5　われわれの開発した小動物専用マイクロSPECT装置

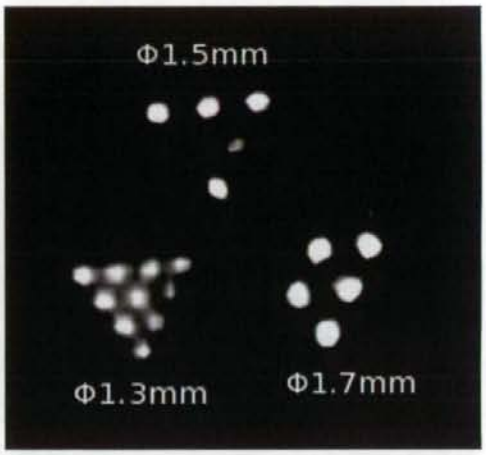

図6　マルチラインソースファントム画像
1.3mm径のラインソースが識別できている。

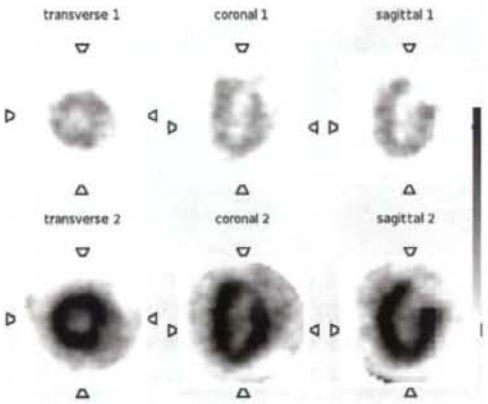

図7　本マイクロSPECT装置で得られた^{201}Tlによるラット心筋SPECT画像の1例
上：安静時、下：負荷時。安静時に対して、負荷時で血流が上昇しているのがわかる。

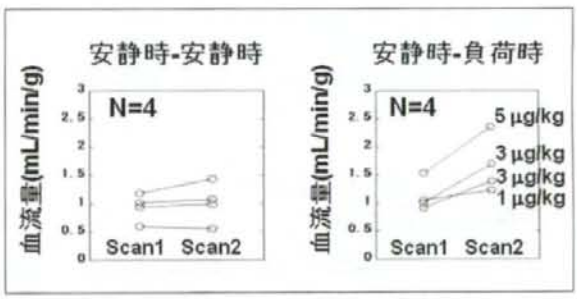

図8　本マイクロSPECT装置で得られた健常ラットの心筋血流量および血管反応性

ンパクトな小動物専用高解像度SPECT装置を開発した（図5）。ピンホールコリメータの欠点でもある低感度を補うことと高感度化のため、被写体の周囲に4台の検出器が90°間隔で配列されている。また、小動物ベッドが水平方向に回転可能となっており、異なる回転軸による撮像軌道で完全データ収集が可能である。

マルチラインソースファントム実験では、1.3mm径のラインが識別可能であった（図6）。また、本装置を用いて、覚醒下で健常ラットの心筋血流量および血管反応性を評価した。^{201}Tlを2回投与して、安静時と安静時、および安静時と血管拡張剤による負荷時の血流量を測定した。図7は本実験で得られたラット心筋SPECT画像であるが、非常に鮮明である。一連の時系列画像を動態解析して血流値が計算され、安静時と安静時では血流値に変化はなく、安静時と負荷時では血管拡張剤の量に依存して血流上昇が確認できた。本装置および画像再構成法によって得られた画像から、ラット心筋血流定量が可能であることが示された（図8）。

ファントムピットマップ	臨床SPECT（パラレルコリメータ＋2D FBP）	ピンホールSPECT、再構成マトリクス：小（従来法）	ピンホールSPECT、再構成マトリクス：大（TC-3DOSEM）
 ピンホール視野			
解像度	低	高	高（2mm FWHM理論値）
定量性	良	過大評価	良

図9　脳ファントムの再構成画像
臨床SPECTでは低解像度で詳細構造は見えない。ピンホールSPECTの局所高解像度撮像では、TC-3DOSEMによる再構成画像にて、従来法で存在していたアーチファクトや過大評価がなく、詳細構造が明瞭に描出されている。

ピンホールSPECTによるヒト局所高解像度撮像

従来、ピンホールSPECTのような小視野検出器でヒトのように大きな被写体を撮像した場合、トランケーションは避けられず、それによるアーチファクトや過大評価により、定量評価は困難であった。トランケーションを許す画像再構成法を利用することで、小動物SPECTで確立したピンホールSPECTによる高解像度撮像技術が、ヒトのように大きな被写体であっても利用でき、局所小領域を拡大した高解像度定量SPECTイメージングが、トランケーションの影響なく可能となる。

ピンホールSPECTによるヒト脳局所高解像度定量撮像の可能性を評価するための物理ファントム実験を行った。ピンホールコリメータを取りつけた臨床用SPECTカメラを固定し、Hoffmanの脳ファントムを回転ステージ上で180°回転させて視野内にファントム外側の領域が含まれるように投影データを収集した。再構成マトリクスが小さい従来法と再構成マトリクスを大きくしたTC-3DOSEMで画像再構成した。また、一般の臨床用SPECTと解像度を比較するため、同じファントムをパラレルホールコリメータでデータ収集し、2D FBP法で画像再構成した。図9に示すように、臨床SPECTでは低解像度で詳細構造は見えなかった。また、ピンホールSPECTデータを従来法で再構成した場合はアーチファクトが見られ、視野全域でカウントが過大評価されていた。一方、ピンホールSPECTデータをTC-3DOSEMで再構成した場合、アーチファクトも過大評価もなく、高解像度で詳細構造が確認できた。

本撮像技術によって、微小腫瘍検出、血管ブラークイメージング、てんかん焦点同定、部分容積効果のない血流定量などが可能になると考えられる。実際に、われわれは図10のような局所高解像度定量SPECT装置を開発中で、脳全域画像と局所高解像度画像を提供する。

おわりに

従来、研究の域を脱しなかったピンホールSPECTは、新しい撮像技術や画像再構成法の開発によって、高解像度かつ定量評価可能な小動物用SPECTとして実用化の域に達した。また、トランケーションを許

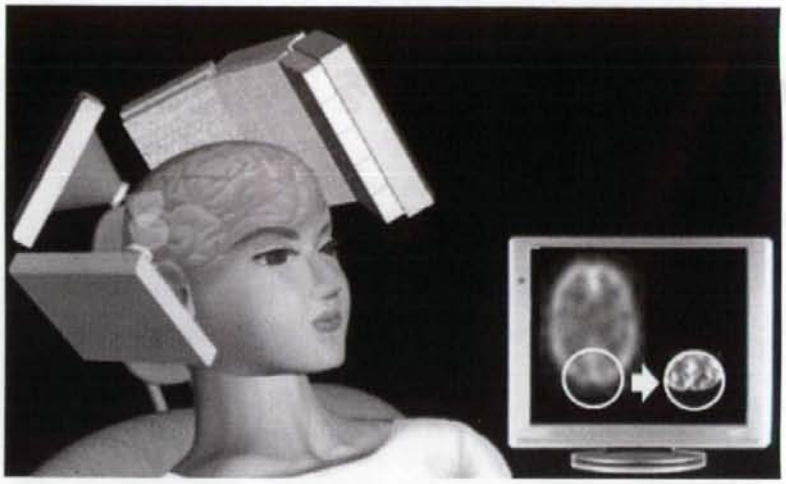

図10　頭部局所高解像度SPECT装置のイメージ図

す画像再構成法によって、ピンホールSPECTを利用したヒトの局所高解像度定量SPECTが開発されようとしている。これまで、解像度が低いといわれてきたSPECT撮像において、新しい撮像技術や画像再構成法などの開発によって高解像度定量撮像が可能になりつつある。

参考文献

1) Meikle SR et al: Small animal SPECT and its place in the matrix of molecular imaging technologies. Phys Med Biol 50(22): R45-61, 2005
2) 間賀田泰寛: 各社製品の性能比較. PET journal (2): 27-29, 2008
3) Vanhove C et al: Interest of the ordered subsets expectation maximization (OS-EM) algorithm in pinhole single-photon emission tomography reconstruction: a phantom study. Eur J Nucl Med 27(2): 140-146, 2000
4) Tuy HK: An inversion formula for cone-beam reconstruction. SIAM J Appl Math 43(3): 546-552, 1982
5) Zeniya T et al: A new reconstruction strategy for image improvement in pinhole SPECT. Eur J Nucl Med Mol Imaging 31(8): 1166-1172, 2004
6) Metzler SD et al: Helical pinhole SPECT for small-animal imaging: a method for addressing sampling completeness. IEEE Trans Nucl Sci 50(5): 1575-1583, 2003
7) Beekman FJ et al: U-SPECT-I: a novel system for submillimeter-resolution tomography with radiolabelled molecules in mice. J Nucl Med 46(7): 1194-1200, 2005
8) Defrise M et al: Truncated Hilbert transform and image reconstruction from limited tomographic data. Inverse Probl 22(3): 1037-1053, 2006
9) Zeniya T et al: 3D-OSEM reconstruction from truncated data in pinhole SPECT. Nuclear Science Symposium Conference Record, 2007. NSS'07. IEEE, 4205-4207
10) Zeniya T et al: Use of a compact pixellated gamma camera for small animal pinhole SPECT imaging. Ann Nucl Med 20(6): 409-416, 2006

Clinical Usability of a Compact High Resolution Detector for High Resolution and Quantitative SPECT Imaging in a Selected Small ROI

Tsutomu Zeniya, Hiroshi Watabe, *Member, IEEE*, Hiroyuki Kudo, *Member, IEEE*, Yoshiyuki Hirano, Kotaro Minato, *Member, IEEE*, and Hidehiro Iida, *Member, IEEE*

Abstract– **SPECT using compact high resolution detector or pinhole collimator allows to image physiological functions with high spatial resolution. However, when field-of-view (FOV) is smaller than the object, the projection data are truncated by radioisotope outside FOV. The truncation causes artifact and overestimation, which decreases quantitative accuracy. Recently Defrise et al proposed a new truncation-compensated reconstruction method, that is, the truncated data can be successfully reconstructed by fulfilling following conditions. First, FOV contains zero or background counts outside the object as known value. Second, reconstructed image space is large enough to contain the whole support of the object. They demonstrated their theory by 2D X-ray CT simulation. This study was aimed at evaluating clinical-SPECT usability of a reconstructed image of a selected small region-of-interest (ROI) with the above Defrise's method. This evaluation was performed by computer simulation with a numerical human brain phantom and a detector with 2-mm resolution, 48-mm FOV and a parallel collimator. The projection data were acquired including the area outside the brain. After adding Gaussian noise, the projection data were reconstructed by maximum likelihood expectation maximization (MLEM) method on the reconstruction matrix large enough to contain the whole support of the brain. This simulation showed that the truncation compensated reconstruction method could provide the image with high resolution and the counts almost equivalent to that of original image in the selected small ROI without the effect of truncation for human brain. In conclusion, this result suggests that a compact high resolution detector can be used for quantitatively reconstructing a selected small ROI with clinical SPECT camera. This technique can also use the pinhole collimator instead of the compact high resolution detector.**

I. Introduction

SPECT using compact high resolution detector or pinhole collimator allows to image physiological functions with high spatial resolution [1]. However, when such a small field-of-view (FOV) detector is applied for a large object like human, the projection data are truncated by radioisotope outside the FOV. The truncation causes artifact and overestimation, which quantitative accuracy. Recently Defrise et al proposed a new truncation-compensated reconstruction method [2]. They demonstrated their theory by 2D X-ray CT simulation. The aim of this study was to evaluate clinical-SPECT usability of a reconstructed image of a selected small region-of-interest (ROI) with the above Defrise's method. This evaluation was performed by 2D computer simulation with a numerical human brain phantom.

II. Materials and Methods

A. Defrise's truncation-compensated reconstruction theory

Defrise's theory compensates the artifact and overestimation due to truncation and exactly reconstructs for FOV, by fulfilling the conditions as shown in Fig. 1. Projection data must be acquired under first condition. And then, the projection data must be reconstructed by iterative reconstruction method such as maximum likelihood expectation maximization (MLEM) method [3] under second condition.

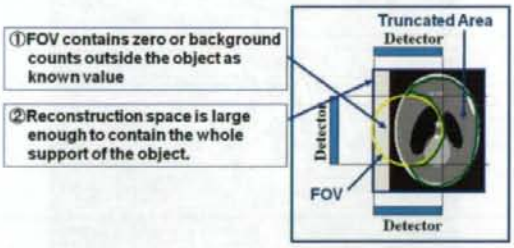

Fig. 1. Conditions to compensated artifact and overestimation due to truncation in Defrise's theory.

B. Computer Simulation

Figure 2 shows the numerical human brain phantom used in this simulation. Image matrix is 90 pixel × 110 pixel. Assuming pixel size of 2 mm, the image size is 180 mm × 220 mm. Pixel values are 1 or 0.

A compact high resolution detector is with 2-mm resolution, 48-mm FOV, 24 bins and a parallel-hole collimator. Projection data for ROI shown by red circle in Fig. 2 were acquired by a circular orbit shown by green line, over 180°,

Manuscript received November 14, 2008. This work was supported in part by the Grant-in-Aid for Scientific Research (B) of the Ministry of Education, Culture, Sports and Technology (20500435), Japan, and the Grant for Translational Research from the Ministry of Health, Labour and Welfare (MHLW), Japan.

T. Zeniya, H. Watabe, Y. Hirano and H. Iida are with the Department of Investigative Radiology, Advanced Medical Engineering Center, National Cardiovascular Center Research Institute, 5-7-1 Fujishirodai, Suita, Osaka 565-8565 Japan (e-mail: zeniya @ri.ncvc.go.jp).

T. Zeniya and K. Minato are with the Graduate School of Information Science, Nara Institute of Science and Technology, Japan.

H. Kudo is with the Department of Computer Science, Graduate School of Systems and Information Engineering, University of Tsukuba, Japan.

978-1-4244-2715-4/08/$25.00 ©2008 IEEE

with 3°step and 60 views. This ROI included the area outside the brain. After adding Gaussian noise, the projection data reconstructed by MLEM method, on the reconstruction matrix of 90 pixel × 110 pixel large enough to contain the whole support of the brain to satisfy the condition of Defrise's theory. To compare with conventional reconstruction method using small reconstruction matrix, projection data with 24 bin were also reconstructed on the reconstruction matrix of 24 pixel × 24 pixel. The number of iteration in MLEM reconstruction was 24 for each method.

To compare with conventional clinical SPECT, untruncated projection data including the whole of the brain were acquired by a 220-mm large FOV (22 bin) detector with low resolution of 10 mm, over 360°, with 3° step and 120 views. After adding Gaussian noise, the projection data were reconstructed by ordered subsets expectation maximization (OSEM) method [4] which is an accelerated MLEM. The OSEM parameters were 8 subsets and 3 iterations.

As reference image, untruncated projection data including the whole of the brain were acquired by a 220-mm large FOV (110 bin) detector with high resolution of 2 mm, over 360°, with 3° step and 120 views. After adding Gaussian noise, the projection data were reconstructed by OSEM method with 8 subsets and 3 iterations. However, this detector is impractical because it is too expensive if manufactured.

The images obtained in this simulation were visually compared, and also the profiles of the images were obtained on line shown by yellow in Fig. 2 to compare quantitatively.

In this simulation, the effects of attenuation, scatter and blurring by collimator were not considered because this simulation was aimed at evaluating truncation-compensated method.

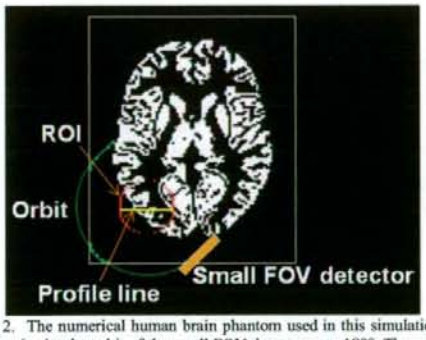

Fig. 2. The numerical human brain phantom used in this simulation. The green line is circular orbit of the small FOV detector over 180°. The red circle is ROI. The yellow line is the position of profiles shown Fig. 4. Pixel values are 1 or 0.

III. Results and Discussion

Figure 3(a) shows the image reconstructed from untruncated projection data using the small FOV detector with low resolution. The obtained image had low resolution. The detail of brain structure was not observed.

Figure 3(b) shows the image reconstructed from untruncated projection data using the large FOV detector with high resolution. The image with high resolution was obtained and the fine structure was observed. However, such a high resolution and large FOV detector is impractical because it is too expensive if manufactured.

Figure 3(c) shows the image reconstructed from truncated projection data obtained using the small FOV detector with high resolution. The projection data were reconstructed on the small reconstruction matrix as conventional reconstruction method. The reconstructed image had artifact and the pixel counts were significantly overestimated.

Figure 3(d) shows the image reconstructed from truncated projection data using the small FOV detector with high resolution. The projection data were reconstructed on the large reconstruction matrix as proposed reconstruction method. The obtained image was with high resolution and the pixel counts almost equivalent to that of original image without the effect of truncation in the selected small ROI.

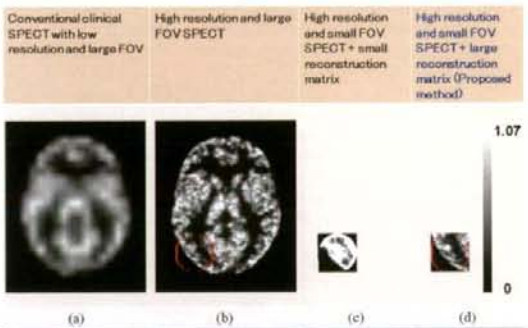

Fig. 3. The reconstructed images obtained in this simulation. All images were displayed with the range of same gray scale [0-1.07] (a) The image obtained from the untruncated projection data of large FOV detector with low resolution as conventional clinical SPECT. (b) The image obtained from the untruncated projection data of large FOV detector with high resolution as the reference image. (c) The image reconstructed from the truncated projection data of small FOV detector with high resolution, on the small reconstruction matrix as conventional reconstruction method. (d) The image reconstructed from the truncated projection data of small FOV detector with high resolution, by the large reconstruction matrix as proposed reconstruction method.

Figure 4 shows the line profiles in a small ROI on the images obtained from the high-resolution detectors. When the truncated projection data from small FOV detector were reconstructed on the small reconstruction matrix, the obtained image had extremely high counts on the edge of and the pixel counts were wholly overestimated. On the other hand, when the truncated projection data from small FOV detector were reconstructed on the large reconstruction matrix, the profile of the image had good agreement with that of the image from the untruncated projection data.

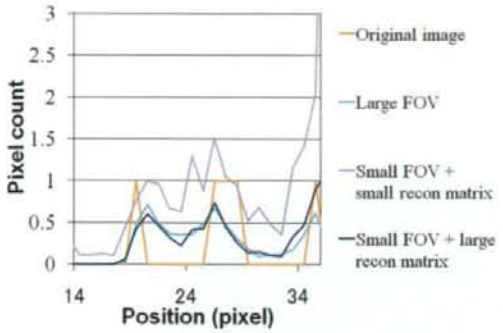

Fig. 4. In a small ROI, the line profiles on the image obtained by reconstructing data from high-resolution detector by each method.

IV. Conclusion

These results suggest that a compact high resolution detector can be used for quantitatively reconstructing a selected small ROI with clinical SPECT camera. This technique can also use the pinhole collimator instead of the compact high resolution detector.

References

[1] S. R. Meikle, P. Kench, M. Kassiou, and R. B. Banati, "Small animal SPECT and its place in the matrix of molecular imaging technologies," *Phys. Med. Biol.*, vol. 50, no. 22, pp. R45-R61, 2005.

[2] M. Defrise, F. Noo, R. Clackdoyle, and H. Kudo, "Truncated Hilbert transform and image reconstruction from limited tomographic data," *Inverse Problems*, vol. 22, no. 3, pp. 1037-1053, 2006.

[3] L. A. Shepp and Y. Vardi, "Maximum likelihood reconstruction for emission tomography," *IEEE Trans. Med. Imaging*, vol. 1, no. 2, pp. 113-122, 1982.

[4] H. M. Hudson and R. S. Larkin, "Accelerated image reconstruction using ordered subsets of projection data," *IEEE Trans. Med. Imaging*, vol. 13, no. 4, pp. 601-609, 1994.

Combination of a High Resolution Detector with Small FOV and a Low Resolution Detector with Large FOV for High Resolution and Quantitative SPECT

Tsutomu Zeniya, Hiroshi Watabe, *Member, IEEE*, Hiroyuki Kudo, *Member, IEEE*, Yoshiyuki Hirano, Kotaro Minato, *Member, IEEE*, and Hidehiro Iida, *Member, IEEE*

Abstract– **SPECT using compact high resolution detector or pinhole collimator allows to image physiological functions with high resolution. However, when region-of-interest (ROI) is smaller than the object, the projection data are truncated due to radioisotope outside ROI. The truncation causes artifact and overestimation, which decrease quantitative accuracy. In theory, to eliminate the artifact and the overestimation due to truncation, the untruncated data from another large field-of-view (FOV) detector can be used even if the detector has low resolution. This study was aimed at evaluating feasibility of combination of a small FOV high resolution detector and a large FOV low resolution detector in clinical circumstance. This evaluation was performed by computer simulation with a numerical torso phantom. We tested whether the image in a selected small ROI (in this case, ROI was heart) can be obtained with high resolution and without artifact and overestimation. The small FOV detector with high resolution was with 1.14-mm resolution, 80-mm FOV and parallel collimator. The whole of heart was included in this FOV, but the surrounding area was truncated. The large FOV detector with low resolution has 9-mm resolution, 360-mm FOV and parallel collimator like conventional clinical SPECT. The untruncated projections including the whole of thorax were acquired by this detector. Gaussian noises were added to all projection data. Data from the small detector were reconstructed by maximum likelihood expectation maximization (MLEM) as iterative method, on the reconstruction matrix large enough to contain the whole of thorax. The reconstructed image from the large FOV detector was used as an initial image in iterative reconstruction. The image obtained by our proposed method had high resolution and the counts almost equivalent to that of original image in the small ROI. In conclusion, this result suggests feasibility of the combination of two detectors with small and large FOV to quantitatively obtain high-resolution image of a selected small ROI with clinical SPECT.**

Manuscript received November 14, 2008. This work was supported in part by the Grant-in-Aid for Scientific Research (B) of the Ministry of Education, Culture, Sports and Technology (20500435), Japan, and the Grant for Translational Research from the Ministry of Health, Labour and Welfare (MHLW), Japan.

T. Zeniya, H. Watabe, Y. Hirano and H. Iida are with the Department of Investigative Radiology, Advanced Medical Engineering Center, National Cardiovascular Center Research Institute, 5-7-1 Fujishirodai, Suita, Osaka 565-8565 Japan (e-mail: zeniya @ri.ncvc.go.jp).

T. Zeniya and K. Minato are with the Graduate School of Information Science, Nara Institute of Science and Technology, Japan.

H. Kudo is with the Department of Computer Science, Graduate School of Systems and Information Engineering, University of Tsukuba, Japan.

I. Introduction

SPECT using compact high resolution detector or pinhole collimator allows to image physiological functions with high spatial resolution [1]. However, when such a small field-of-view (FOV) detector is applied for a large object like human, the projection data are truncated by radioisotope outside region-of-interest (ROI). The truncation causes artifact and overestimation, which quantitative accuracy. Truncation-compensated reconstruction theory proposed by Defrise et al uses area outside the object with ROI as a prior knowledge to solve the truncation problem [2]. Defrise's theory can't be applied for the case that ROI does not contain the area outside the object. The aim of this study was to evaluate feasibility fo combination of a small-FOV high-resolution detector and a large-FOV low-resolution detector in clinical circumstance. We tested whether the image in a selected small ROI (in this case, ROI was heart) can be reconstructed with high resolution and without the effect of truncation by using untruncated data from the large FOV detector, which do not need to have high resolution, even if ROI in small FOV detector with high resolution does not contain the area outside the object. This evaluation was performed by 2D computer simulation with a numerical human torso phantom.

II. Materials and Methods

A. Support from large-FOV low-resolution detector for truncation problem

As shown in Fig. 1, our proposed method uses untruncated data from the large FOV detector with low resolution, in order to compensate the artifact and overestimation due to truncation in small FOV detector.

Our proposed approach based on iterative reconstruction method such as maximum likelihood expectation-maximization (MLEM) [3] or ordered-subsets expectation-maximization (OSEM) [4] algorithm is, as follows:

Step1: the object is reconstructed using OSEM from untruncated data of the large FOV detector with high resolution;

Step2: In the MLEM reconstruction, the image reconstructed from the large FOV detector is used as initial

978-1-4244-2715-4/08/$25.00 ©2008 IEEE

reference image and forward-projected, and the reconstruction matrix is large enough to contain the whole object;

Step3: Truncated data from small FOV detector are used as real projection in the MLEM reconstruction process.

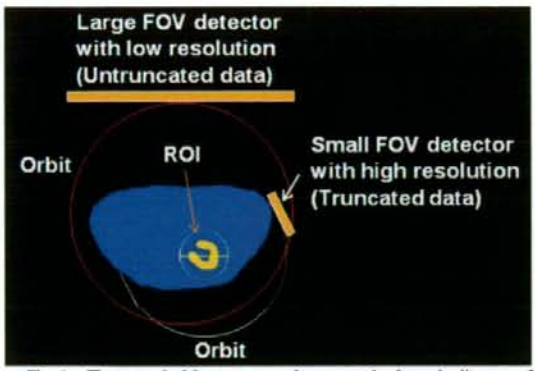

Fig. 1. The numerical human torso phantom and schematic diagram of SPECT system with two kinds of detectors. Untruncated data from low-resolution detector with large FOV are used to compensate the artifact and overestimation due to truncation in small FOV detector. The white line shows the small FOV detector and its circular orbit over 180° to image heart with high resolution. The red line shows the large FOV detector and its circular orbit over 360° to acquire untruncated projection data.

B. Computer Simulation

This simulation was performed using the numerical human torso phantom as shown in Fig. 1. Image matrix is 256 pixels × 320 pixels. Assuming pixel size of 1.14 mm, image size 360 mm × 290 mm. Pixel values are 3 and 1 for heart and the surrounding area.

The small FOV detector with high resolution has 1.14-mm resolution, 80-mm FOV and parallel collimator. The whole of heart was included in this FOV, but the surrounding area was truncated. Projection data of ROI shown by white circle in Fig. 1 were acquired by a circular orbit shown by white line, over 180°, with 3°step and 60 views. The large FOV detector with low resolution has 9-mm resolution, 360-mm FOV and parallel collimator like conventional clinical SPECT. The projections data including the whole of thorax were acquired without truncation by this large FOV detector. A red circle in Fig. 1 shows orbit of the large FOV detector. Projection data were acquired with 3° step and 120 views over 360°. Gaussian noises were added to all projection data. Data from the small FOV detector were reconstructed by MLEM method as iterative reconstruction method, on the reconstruction matrix of 256 pixels ×320 pixels large enough to contain the whole of thorax. The reconstructed image from the large FOV detector was used as an initial image in iterative reconstruction. To compare with conventional reconstruction method, projection data with 70 bins were reconstructed on the reconstruction matrix of 70 pixels ×70 pixels. The number of iteration in MLEM reconstruction was 16.

To compare with conventional clinical SPECT, untruncated projection data including the whole of the brain were acquired by a 360-mm FOV (40 bin) detector with low resolution of 9 mm, over 360°, with 3° step and 120 views. After adding Gaussian noise, the projection data were reconstructed by OSEM method as one of iterative reconstruction method, with 8 subsets and 2 iterations.

As reference image, untruncated projection data including the whole of the brain were acquired by a 360-mm FOV (320 bin) detector with high resolution of 1.14 mm, over 360°, with 3° step and 120 views. After adding Gaussian noise, the projection data were reconstructed by OSEM method as one of iterative reconstruction method, with 8 subsets and 2 iterations. However, this detector is impractical because it is too expensive if manufactured.

The images obtained in this simulation were visually compared, and also the profiles of the images were obtained on straight line over heart shown in Fig. 1 to compare quantitatively.

In this simulation, the effects of attenuation, scatter and blurring by collimator were not considered because this simulation was aimed at evaluating truncation-compensated method.

Furthermore, we evaluated the rotating angle in the orbit of small FOV detector. Small rotating angle is desirable because the detector can be closer to the object when the rotating angle is smaller as shown in Fig. 2. Therefore, the small rotating angle improves the sensitivity and the resolution. The rotating angles of 45 °, 90°, 120°, 150° and 180° were tested. All projection data were reconstructed by our proposed method.

Fig. 2. The orbits of the detector according to the rotating angles. White lines are the orbits of detector. The rotating angle is 180° for the outermost orbit. The rotating angle is 45° for the innermost orbit.

III. Results and Discussion

Figure 3(a) shows the image reconstructed from untruncated projection data using the small FOV detector with low resolution. The obtained image had low resolution. The heart was blurred.

Figure 3(b) shows the image reconstructed from untruncated projection data using the large FOV detector with high resolution. The clear image with high resolution was obtained. However, such a high resolution and large FOV detector is impractical because it is too expensive if manufactured.

Figure 3(c) shows the image reconstructed from truncated projection data obtained using the small FOV detector with high resolution. The projection data were reconstructed on the small reconstruction matrix as conventional reconstruction

method. The reconstructed image had artifact and the pixel counts were significantly overestimated.

Figure 3(d) shows the image reconstructed from truncated projection data using the small FOV detector with high resolution. The projection data were reconstructed by proposed reconstruction method. In the small ROI, the clear image with high resolution was obtained without the artifact and the overestimation, and was almost equivalent to the image from the large FOV detector with high resolution.

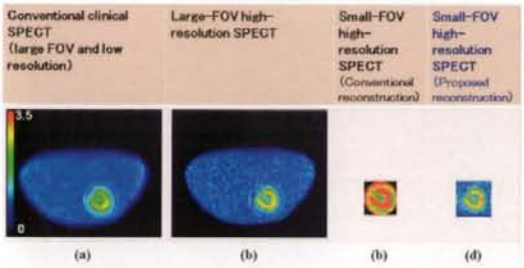

Fig. 3. The reconstructed images obtained in this simulation. All images were displayed with the range of same gray scale [0-3.5] (a) The image obtained from the untruncated projection data of large FOV detector with low resolution as conventional clinical SPECT. (b) The image obtained from the untruncated projection data of large FOV detector with high resolution as the reference image. (c) The image reconstructed from the truncated projection data by small FOV detector with high resolution, on the small reconstruction matrix as conventional reconstruction method. (d) The image reconstructed from the truncated projection data of small FOV detector with high resolution, by proposed reconstruction method.

Figure 4 shows the line profiles in a small ROI on the images obtained from the high-resolution detectors. When the truncated projection data from small FOV detector were reconstructed on the small reconstruction matrix, the obtained image had extremely high counts on the edge of ROI and the pixel counts were wholly overestimated. On the other hand, when the truncated projection data from small FOV detector were reconstructed by our proposed method, the profile of the image had good agreement with that of the image from the untruncated projection data.

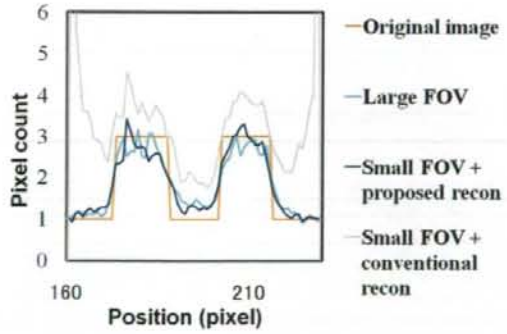

Fig. 4. In a small ROI, the line profiles on the image obtained by reconstructing data from high-resolution detector by each method.

Figure 5 shows the images obtained from projection data acquired by various rotating angles. The image by rotating angle of 150° was almost equivalent to that by rotating angle of 180°. However, the shapes of the hearts were distorted in the images by the rotating angles less than 120°. Usability of the rotating angle of 150° was suggested instead of 180°

Fig. 5. The images reconstructed from projection data acquired by various rotating angles. When the rotating angle is smaller, the radius of rotation can be smaller.

IV. Conclusion

These results suggested feasibility of the combination of two kinds of detectors with small and large FOVs quantitatively obtain high resolution image of a selected small ROI with clinical SPECT. In other words, the image in a selected small ROI can be reconstructed with high resolution and without the effect of truncation by using untruncated data from the large FOV detector, which do not need to have high resolution, even if ROI in small FOV detector with high resolution does not contain the area outside the object.

References

[1] S. R. Meikle, P. Kench, M. Kassiou, and R. B. Banati, "Small animal SPECT and its place in the matrix of molecular imaging technologies," *Phys. Med. Biol.*, vol. 50, no. 22, pp. R45-R61, 2005.

[2] M. Defrise, F. Noo, R. Clackdoyle, and H. Kudo, "Truncated Hilbert transform and image reconstruction from limited tomographic data," *Inverse Problems*, vol. 22, no. 3, pp. 1037-1053, 2006.

[3] L. A. Shepp and Y. Vardi, "Maximum likelihood reconstruction for emission tomography," *IEEE Trans. Med. Imaging*, vol. 1, no. 2, pp. 113-122, 1982.

[4] H. M. Hudson and R. S. Larkin, "Accelerated image reconstruction using ordered subsets of projection data," *IEEE Trans. Med. Imaging*, vol. 13, no. 4, pp. 601-609, 1994.

Circ J 2007; **71:** 1035–1039

Are Cardiac Events During Exercise Therapy for Heart Failure Predictable From the Baseline Variables?

Isao Nishi, MD; Teruo Noguchi, MD; Shinichi Furuichi, MD; Yoshitaka Iwanaga, MD; Jiyoong Kim, MD; Hideo Ohya, MD; Naohiko Aihara, MD; Hiroshi Takaki, MD; Yoichi Goto, MD

Background Exercise training (ET) is an emerging therapy for chronic heart failure, but the baseline patient characteristics for predicting cardiac events (CEs) during the course of ET remain unknown.

Methods and Results Of the 111 stable heart failure patients who participated in a 3-month ET program, 6 withdrew from the program for cardiac reasons and 9 had transient interruptions in the program because of CEs. The baseline clinical characteristics of these 15 patients (CE group) and the remaining 96 patients (No-CE group) were compared. Compared with the No-CE group, the CE group had a significantly higher prevalence of pacemaker/implantable cardioverter-defibrillators, larger left ventricular end-diastolic diameter (LVEDDs), lower peak oxygen uptake, greater ventilation drive, and higher plasma brain natriuretic peptide concentration at baseline. Multivariate logistic regression analysis showed that a larger LVEDD was a significant predictor of the occurrence of a transient interruption to or permanent withdrawal from the ET program because of CEs. Receiver operating characteristic curve analysis demonstrated that an LVEDD ≥65 mm had a sensitivity of 93% and specificity of 48% in predicting CEs.

Conclusions Patients with a large LVEDD (≥65 mm) at baseline should be monitored carefully during the course of an ET program. (*Circ J* 2007; **71:** 1035–1039)

Key Words: Cardiac events; Cardiac rehabilitation; Chronic heart failure; Exercise training; Predictors

Recent clinical studies have demonstrated that exercise training (ET) improves functional status, quality of life, and prognosis of patients with chronic heart failure[1–4] Because restricted physical activity promotes physical deconditioning, which may adversely affect the clinical status of a patient and exacerbate the exercise intolerance of patients with chronic heart failure, ET is recommended as an adjunct to improving the clinical status of ambulatory patients with current or prior symptoms of heart failure and a reduced left ventricular ejection fraction (LVEF).[5] As might be expected, there are populations of patients with chronic heart failure who transiently interrupt or permanently withdraw from ET programs because of cardiac events (CE). Although we have reported that the rate of permanent withdrawal from such programs because of cardiac problems is approximately 5%,[6] other patients may have a transient interruption to their ET for reasons such as a transient worsening of the heart failure or arrhythmias. Only a few reports, however, have investigated the characteristics of patients with chronic heart failure who are likely to transiently interrupt or permanently withdraw from an exercise program.[7] Thus, it remains unclear which subgroup of patients with chronic heart failure is likely to experience these problems and if the predictors of these problems could be identified, ET for patients with heart failure would be safer and more effective.

(Received July 18, 2006; revised manuscript received April 9, 2007; accepted April 19, 2007)

Division of Cardiology, National Cardiovascular Center, Suita, Japan
Mailing address: Yoichi Goto, MD, Division of Cardiology, National Cardiovascular Center, 5-7-1 Fujishiro-dai, Suita 565-8565, Japan. E-mail: ygoto@hsp.ncvc.go.jp

Accordingly, the purpose of the present study was to identify such predictors. To this end, we used multivariate analysis to compare the baseline clinical characteristics of patients who did or did not transiently interrupt or permanently withdraw from an exercise program.

Methods

Patients

The entry criteria for our exercise cardiac rehabilitation program for heart failure were: aged 15–80 years, left ventricular (LV) systolic dysfunction with an LVEF ≤40%, reduced exercise tolerance, a well-controlled body fluid level (euvolemic), and no signs of worsening of heart failure during the past fortnight. LVEF was determined from left ventriculography using contrast medium or radioisotope. A total of 111 patients with heart failure participated in the program and all gave informed consent to the protocol. The clinical characteristics of the patients were as follows: 85% male, between 19 and 72 years old, 98% began as inpatients, and New York Heart Association classes I–III.

The Cardiac Rehabilitation Program

The cardiac rehabilitation program for chronic heart failure was developed by modifying a previously reported program for acute myocardial infarction.[8–12] Patients were enrolled in the ET program when they did not have ischemic changes on electrocardiography (ECG) or severe arrhythmia during an initial submaximal exercise test (a 6-min walking test or a treadmill walking test with 0% slope up to 75% of the predicted maximal heart rate (HR) or to level 15 ["hard"] of the 6–20 scale rating of perceived exertion).

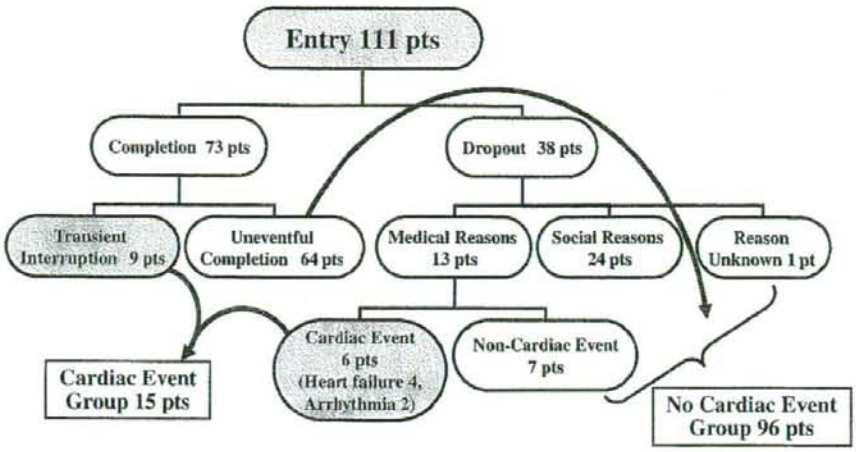

Fig 1. Patient classification by clinical course during the exercise training program for chronic heart failure. pts, patients.

The exercise program consisted of walking, bicycling on an ergometer, and calisthenics for 40–60 min/session and 3–5 sessions/week for 3 months. Exercise intensity was determined individually at 30–50% of HR reserve (Karvonen's equation: k=0.3–0.5);[13] an anaerobic threshold (AT) level obtained in a maximal symptom-limited cardiopulmonary exercise test, or at levels 11–13 ("fairly light" to "somewhat hard") of the 6–20 scale rating of perceived exertion (the original Borg's score[14]). Care was taken to prescribe a slightly lower level of exercise intensity (30–40% of HR reserve or an AT level) and lower session frequency (3 sessions/week) to patients with a very low LVEF (<20%). The exercise program usually began with supervised sessions for 2–4 weeks, followed by home exercise combined with once or twice weekly supervised sessions for the remaining 8–10 weeks. Home exercise consisted mainly of brisk walking at a prescribed HR for 30–50 min, 3–5 times per week.

Patients were encouraged to attend education classes, which were held 3 times each week, with lectures given by physicians, nurses, dieticians, and pharmacists on coronary artery diseases, secondary prevention, heart failure management, diet, smoking cessation, and medication. In addition, all patients received individual counseling on exercise prescription, secondary prevention, and daily life activities by a physician and a nurse at the time of hospital discharge and at the end of the 3-month cardiac rehabilitation program.

Cardiopulmonary Exercise Testing

Patients were scheduled to undergo a symptom-limited cardiopulmonary exercise test at the beginning and the end of the 3-month cardiac rehabilitation program. After a 2-min rest on the bicycle ergometer in the upright position, the patient started pedaling at an intensity of 0 W for 1 min (warm-up), and then performed an incremental exercise test with a ramp protocol (10 or 15 W/min) until exhaustion. Twelve-lead ECG was continuously monitored and blood pressure was measured every minute with a sphygmomanometer. Expired gas was collected and analyzed continuously with an AE-280S or AE-300S gas analyzer (Minato Co, Osaka, Japan). Peak oxygen uptake (peak $\dot{V}O_2$) was defined as the highest $\dot{V}O_2$ value achieved at peak exercise. Ventilation ($\dot{V}E$) and carbon dioxide output ($\dot{V}CO_2$) were measured and the gradient of the $\dot{V}E$-$\dot{V}CO_2$ relationship ($\dot{V}E/\dot{V}CO_2$ slope) was determined.

Echocardiography

All 111 patients underwent echocardiography before the entry into the ET program. LV internal diameters were acquired from the parasternal short-axis view, approximately at the mitral chordae level, using direct 2-dimensional measurements or targeted M-mode echocardiography provided that the M-mode cursor can be positioned perpendicular to the septum and LV posterior wall.

Clinical Course and Patient Categories

Of the 111 patients, 73 patients completed the 3-month cardiac rehabilitation program and 38 did not (ie, permanent withdrawal). Of these 38 patients, 24 gave social reasons (the distance to the institute was too far, return to work etc), 7 had non-cardiac medical reasons (lumbago, claudication etc), 6 experienced cardiac problems, and 1 left for an unknown reason (Fig 1). The cardiac reasons provided by the 6 patients were exacerbation of the heart failure (n=4), ventricular tachycardia (n=1), and atrial fibrillation (n=1). Of the 73 patients who completed the program, 9 transiently interrupted the ET for cardiac reasons, including exacerbation of heart failure (n=2), implantation of an implantable cardioverter-defibrillator (ICD) to address ventricular fibrillation (n=1), discharges of ICD shocks for ventricular tachycardia (n=1), occurrence of ventricular tachycardia (n=2), implantation of a pacemaker (n=1), more coronary artery bypass surgery (n=1), and hypotension (n=1).

The patients who transiently interrupted their ET (n=9) and those who permanently withdrew from the program (n=6) for cardiac reasons were categorized together as the CE group (n=15), and the remaining patients were categorized as the no-CE group (n=96). We categorized the 24 patients who permanently withdrew for social reasons into the no-CE group because our previous study[6] indicated that there were no differences in baseline clinical data, includ-

Table 1 Clinical Characteristics and Baseline Data of the 2 Groups

	Cardiac event (n=15)	No cardiac event (n=96)	p value
Age (years)	52±12	50±13	NS
Male (%)	87	84	NS
NYHA class (I/II/III) (%)	0/20/80	8/41/51	NS
DCM/IsCM/Others (%)	47/40/13	60/20/20	NS
Pacemaker/ICD (%)	27	7	<0.05
HT (%)	20	35	NS
HL (%)	40	41	NS
IGT/DM (%)	47	31	NS
Body mass index	20.9±3.6	22.7±4.6	NS
Medication			
Digitalis (%)	80	68	NS
Diuretics (%)	93	88	NS
ACEI/ARB (%)	80	96	NS
β-blocker (%)	93	92	NS
Ca antagonist (%)	7	13	NS
Nitrate (%)	33	17	NS
Cardiotonic (%)	47	23	NS
Antiarrhythmic agent (%)	60	36	NS
Baseline data			
BNP (pg/ml)	437±270	216±266	<0.01
LVEDD (mm)	75±9	66±8	<0.001
LVEF (%)	22±7	25±8	NS
Peak $\dot{V}O_2$ (ml/min)	899±409	1,228±438	<0.05
Peak $\dot{V}O_2$ % predict (%)	47.1±13.3	59.6±13.7	<0.01
$\dot{V}E/\dot{V}CO_2$ slope	37.8±10.2	29.8±7.5	<0.001

NYHA, New York Heart Association; DCM, dilated cardiomyopathy; IsCM, ischemic cardiomyopathy; ICD, implantable cardioverter-defibrillator; HT, hypertension; HL, hyperlipidemia; IGT, impaired glucose tolerance; DM, diabetes mellitus; ACEI, angiotensin-converting enzyme inhibitors; ARB, angiotensin II receptor blocker; BNP, B-type natriuretic peptide; LVEDD, left ventricular end-diastolic diameter; LVEF, left ventricular ejection fraction; $\dot{V}O_2$, oxygen uptake; $\dot{V}E$, ventilation; $\dot{V}CO_2$, carbon dioxide output. Data are mean±SD. BNP data, the peak $\dot{V}O_2$ data, and the $\dot{V}E/\dot{V}CO_2$ slope data were available for only 110, 105, and 104 patients, respectively.

Table 2 Predictors of Cardiac Events by Multivariate Analysis

	OR	p value	95%CI
Pacemaker/ICD	1.485	0.678	0.230–9.592
BNP (pg/ml)	1.000	0.834	0.998–1.003
LVEDD (mm)	1.085	0.044	1.002–1.175
Peak $\dot{V}O_2$ (ml/min)	0.998	0.179	0.996–1.001
$\dot{V}E/\dot{V}CO_2$ slope	1.039	0.489	0.933–1.157

OR, odds ratio; CI, confidence interval. Other abbreviations as in Table 1.

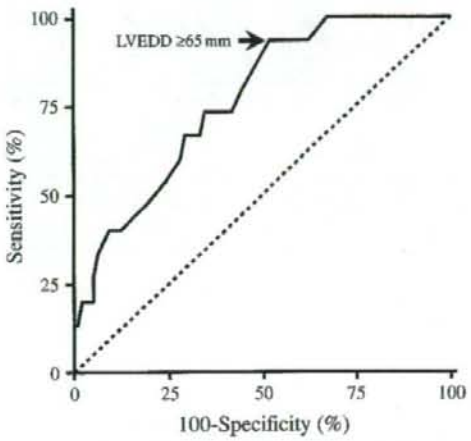

Fig 2. Receiver operating characteristic curve analysis for the left ventricular end-diastolic diameter (LVEDD) as a predictor of cardiac events during the exercise program. The LVEDD cutoff value of ≥65 mm resulted in a sensitivity of 93.3% and specificity of 47.9%.

ing plasma B-type natriuretic peptide (BNP) level, LV dimensions, LVEF, and exercise capacity between them and patients with uneventful completion. Baseline clinical data were compared between the 2 groups to identify predictors of transient interruption or permanent withdrawal for cardiac reasons during the course of the 3-month cardiac rehabilitation program.

Statistical Analysis

Data are presented as the mean±standard deviation. Significant differences were determined by paired or unpaired t-tests where appropriate. Differences in frequencies were analyzed with the Fisher exact probability test or the chi-squared test. Multivariate logistic regression analysis was performed to determine the significant predictors of transient interruption in or permanent withdrawal from the ET program because of CEs. Significant variables detected using an unpaired t-test, the Fisher exact probability test, or chi-squared test were included in the multivariate analysis. Then, receiver operating characteristic (ROC) curve analysis was performed to determine the best cutoff value that predicted the CE with the largest sum of sensitivity and specificity. Statistical calculations were performed using Statview or SPSS software (Chicago, IL, USA). A p-value less than 0.05 was considered statistically significant.

Results

Ninety patients (10 of the 15 patients in the CE group and 80 of the 96 patients in the no-CE group) completed a symptom-limited cardiopulmonary exercise test at the beginning and end of the program. In these patients, peak $\dot{V}O_2$ increased significantly from 1,227±452 to 1,372±527 ml/min ($p<0.001$), and the $\dot{V}E/\dot{V}CO_2$ slope marginally decreased (29.8±8.0 to 28.8±7.7, $p=0.058$) after ET.

Table 1 summarizes the clinical characteristics of the patients and the baseline data for LV function and exercise tolerance in both groups. Compared with the no-CE group, the CE group had a significantly higher prevalence of pacemakers/ICDs (27 vs 7%, $p<0.05$), larger LV end-diastolic diameter (LVEDD) (75±9 vs 66±8 mm, $p<0.01$), lower peak $\dot{V}O_2$ (899±409 vs 1,228±438 ml/min, $p<0.05$; 47±13 vs 60±14%, $p<0.01$), greater ventilation drive ($\dot{V}E/\dot{V}CO_2$ slope: 37.8±10.2 vs 29.8±7.5, $p<0.01$), and higher plasma BNP concentration (437±270 vs 216±266 pg/ml, $p<0.01$).

Multivariate logistic regression analysis, which incorporated pacemaker/ICD implantation, LVEDD, peak $\dot{V}O_2$, $\dot{V}E/\dot{V}CO_2$ slope, and plasma BNP concentration, demonstrated that a larger LVEDD (odds ratio: 1.085, confidence interval: 1.002–1.175) was a significant independent predictor of a transient interruption in or permanent withdrawal from the ET program for cardiac reasons (Table 2).

The ROC curve analysis indicated that a cutoff level of

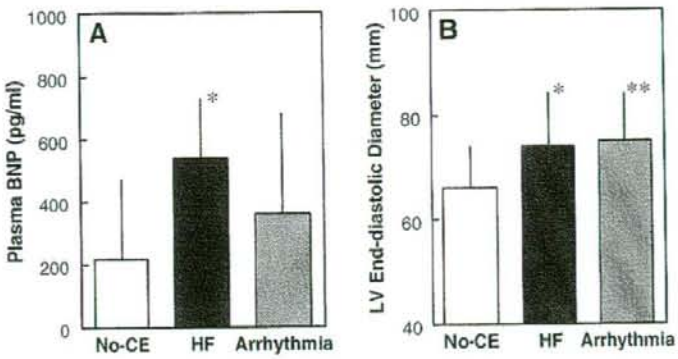

Fig 3. (A) Comparison of plasma B-type natriuretic peptide (BNP) levels among 96 patients with no cardiac events (No-CE), 7 patients with heart failure (HF) exacerbation/hypotension, and 7 patients with arrhythmic events. (B) Comparison of left ventricular (LV) end-diastolic diameter among the same 3 groups as in panel A. *p<0.05, **p<0.01 compared with No-CE group.

LVEDD ≥65 mm best predicted CE, with a sensitivity of 93.3% and specificity of 47.9% (Fig 2). In addition, this criterion of LVEDD ≥65 mm had a positive predictive value of 21.9% and negative predictive value of 97.9% in the present patient population.

No serious CE, such as death or cardiopulmonary arrest, occurred during the ET sessions.

Discussion

Major Findings

The major finding of the present study was that the predictors of the occurrence of CE causing either a transient interruption or permanent withdrawal during the course of the 3-month ET program for chronic heart failure were: pacemaker/ICD implantation, larger LVEDD, lower exercise tolerance, greater ventilation drive, and higher plasma BNP concentration at baseline. In addition, multivariate analysis indicated that a large LVEDD was an independent predictor of CE during the ET program.

Previous Studies

Vanhees et al reported that 4 of 106 patients with an ICD decided to terminate rehabilitation after receiving shocks for ventricular tachycardia![5] In the present patients, all of whom had a poorly functioning LV, 3 of 7 patients with an ICD experienced shocks for ventricular tachycardia or refractory ventricular tachycardia. Therefore, chronic heart failure patients with implanted pacemakers/ICDs seem to be more likely to develop CE while participating in an ET program. However, ET with an appropriate prescription and careful supervision, rather than restriction of exercise, may be the recommended course of treatment for these patients, because cardiac rehabilitation with ET has been reported to improve exercise capacity and quality of life in patients with ICDs![6]

Webb-Peploe et al demonstrated that complications from ET were more common in patients with ischemic cardiomyopathy, larger LV diameters, reduced fractional shortening, earlier peak mitral flow, lower exercise tolerance, and greater ventilation drive at baseline[7] Although the present results, which show that a larger LV diameter, lower exercise tolerance, and greater ventilation drive were predictors of CE, agree with the results reported by Webb-Peploe et al, an ischemic origin and reduced LV contractile function were not identified by us as significant predictors of CE. This discrepancy may be explained by differences in the type of exercise program (home-based exercise in their study vs supervised exercise in the present study), the exercise intensity (70–80% of maximum HR vs 30–50% of HR reserve in the present study), and more importantly, the proportion of patients taking β-blockers (4% vs 92% in the present study). Thus, the present results may be more relevant for ET in patients with chronic heart failure in the current era of widely used β-blockers.

Present Study

Using multivariate analysis, we demonstrated that a larger LVEDD predicts that the patient is at high risk for transiently interrupting or permanently withdrawing from an ET for cardiac reasons. In addition, ROC curve analysis identified the best LVEDD cutoff level to be ≥65 mm. Although the specificity (47.9%) of the criterion of an LVEDD ≥65 mm was low, the sensitivity (93.3%) and negative predictive value (97.9%) were very high. This indicates that if a patient with heart failure has an LVEDD <65 mm, the risk is low that they will discontinue the ET program transiently or permanently for cardiac reasons. This criterion should help stratify heart failure patients before they start the ET program.

Why Does LVEDD Represent the Best Predictor?

In the present study, exacerbation of heart failure or hypotension (n=7) and arrhythmic events (n=7) were the main causative factors among the 15 patients who transiently interrupted or permanently withdrew because of CE. We consider that the reason why LVEDD represents the best predictor among the univariate predictors to be as follows. Compared with the 96 patients in the no-CE group, the 7 patients with heart failure exacerbation/hypotension had significantly higher plasma BNP levels at baseline (539±199 vs 216±266 pg/ml, p<0.05 by Scheffe's method), whereas no significant difference was noted between the 7 patients with arrhythmic events and the no-CE group (360±325 vs 216±266 pg/ml, NS) (Fig 3). On the other hand, LVEDD at baseline in the 7 patients with heart failure exacerbation/hypotension (74±11 mm, p<0.05) and the 7 patients with arrhythmic events (75±9 mm, p<0.01) was significantly greater than that in the no-CE group (66±8 mm). These findings suggest that the baseline plasma BNP concentration can predict exacerbation of heart failure, but not arrhythmic events, leaving the LVEDD as an independent index capable of predicting both events. Although this finding appears to disagree with the study of Berger R et al[17] who demon-

strated that BNP was a predictor of sudden death in patients with chronic heart failure, the differences in patient population, therapeutic interventions, and the clinical endpoints between the 2 studies may explain the disagreement.

Study Limitations

This retrospective study took place in a single center and the total numbers of patients and events were not large. The study, however, reflects the common practices for cardiac patients more accurately than a controlled randomized study.

One potential confounder in the present study might be the combined categorization of uneventful completion patients and social dropout patients into the same "no-CE group". However, an additional analysis of comparison between the uneventful completion group (n=64) and the CE group (n=15) yielded similar results to the original analysis; the CE group had a higher prevalence of pacemakers/ICD implantations (27 vs 5%, $p<0.05$), larger LVEDD (75±9 vs 67±8 mm, $p<0.01$), lower peak $\dot{V}O_2$ (899±409 vs 1,247±448 ml/min, $p<0.05$; 47±13 vs 60±14%, $p<0.01$), greater ventilation drive ($\dot{V}E/\dot{V}CO_2$ slope: 37.8±10.2 vs 29.2±7.7, $p<0.01$), and higher plasma BNP concentrations (437±270 vs 241±314 pg/ml, $p<0.05$) than the uneventful completion group. Therefore, the inclusion of the social dropout patients into no-CE group would not compromise the present results.

Because we did not have a control heart failure group that did not undergo ET, we could not determine whether or not the CE were precipitated by the ET. This, however, is not a major concern because the main scope of the present study was to determine from the baseline data predictors of CE during the ET, regardless of the cause of the CE. With regard to whether or not ET precipitates CE, previous meta-analyses of prospective randomized studies have demonstrated that ET reduces the number of major CE in patients with heart failure![8]

Conclusion

Patients who experience CE during ET programs characteristically have an implanted pacemaker/ICD, larger LV diameter, lower exercise tolerance, greater ventilation drive, and higher plasma BNP concentration. In particular, because LVEDD is an independent predictor of CEs, patients with a large LVEDD (≥65 mm) should be monitored carefully during the course of an ET program.

Acknowledgments

Supported in part by a Research Grant for Cardiovascular Diseases (15A-2) and Health and Labor Sciences Research Grant (H19-011) from the Ministry of Health, Labor and Welfare, Japan.

References

1. European Heart Failure Training Group. Experience from controlled trials of physical training in chronic heart failure: Protocol and patient factors in effectiveness in the improvement in exercise tolerance. *Eur Heart J* 1998; **19:** 466–475.
2. Hambrecht R, Fiehn E, Weigl C, Gielen S, Hamann C, Kaiser R, et al. Regular physical exercise corrects endothelial dysfunction and improves exercise capacity in patients with chronic heart failure. *Circulation* 1998; **98:** 2709–2715.
3. Belardinelli R, Georgiou D, Cianci G, Purcaro A. Randomized, controlled trial of long-term moderate exercise training in chronic heart failure: Effects on functional capacity, quality of life, and clinical outcome. *Circulation* 1999; **99:** 1173–1182.
4. Working Group on Cardiac Rehabilitation & Exercice Physiology and Working Group on Heart Failure of the European Society of Cardiology. Recommendations for exercise training in chronic heart failure patients. *Eur Heart J* 2001; **22:** 125–135.
5. Hunt SA, Abraham WT, Chin MH, Feldman AM, Francis GS, Ganiats TG, et al; American College of Cardiology; American Heart Association Task Force on Practice Guidelines; American College of Chest Physicians; International Society for Heart and Lung Transplantation; Heart Rhythm Society. ACC/AHA 2005 Guideline Update for the Diagnosis and Management of Chronic Heart Failure in the Adult: A report of the American College of Cardiology/American Heart Association Task Force on Practice Guidelines (Writing Committee to Update the 2001 Guidelines for the Evaluation and Management of Heart Failure): Developed in collaboration with the American College of Chest Physicians and the International Society for Heart and Lung Transplantation: Endorsed by the Heart Rhythm Society. *Circulation* 2005; **112:** 1825–1852.
6. Nishi I, Furuichi S, Iwanaga Y, Noguchi T, Kim J, Ohya H, et al. The incidence and reasons for withdrawal from exercise training program in patients with chronic heart failure. *J Jpn Assoc Card Rehab* 2005; **10:** 267–271 (in Japanese).
7. Webb-Peploe KM, Chua TP, Harrington D, Henein MY, Gibson DG, Coats AJ. Different response of patients with idiopathic and ischaemic dilated cardiomyopathy to exercise training. *Int J Cardiol* 2000; **74:** 215–224.
8. Otsuka Y, Takaki H, Okano Y, Satoh T, Aihara N, Matsumoto T, et al. Exercise training without ventricular remodeling in patients with moderate to severe left ventricular dysfunction early after acute myocardial infarction. *Int J Cardiol* 2003; **87:** 237–244.
9. Sakuragi S, Takagi S, Suzuki S, Sakamaki F, Takaki H, Aihara N, et al. Patients with large myocardial infarction gain a greater improvement in exercise capacity after exercise training than those with small to medium infarction. *Clin Cardiol* 2003; **26:** 280–286.
10. Takagi S, Sakuragi S, Baba T, Takaki H, Aihara N, Yasumura Y, et al. Predictors of left ventricular remodeling in patients with acute myocardial infarction participating in cardiac rehabilitation: Brain natriuretic peptide and anterior infarction. *Circ J* 2004; **68:** 214–219.
11. Iwanaga Y, Nishi I, Ono K, Takagi S, Tsutsumi Y, Ozaki M, et al. Angiotensin-converting enzyme genotype is not associated with exercise capacity or the training effect of cardiac rehabilitation in patients after acute myocardial infarction. *Circ J* 2005; **69:** 1315–1319.
12. Suzuki S, Takaki H, Yasumura Y, Sakuragi S, Takagi S, Tsutsumi Y, et al. Assessment of quality of life with 5 different scales in patients participating in comprehensive cardiac rehabilitation after acute myocardial infarction. *Circ J* 2005; **69:** 1527–1534.
13. Karvonen M, Kentala K, Mustala O. The effects of training on heart rate: A longitudinal study. *Ann Med Exp Biol Fenn* 1957; **35:** 307–315.
14. Borg G. Perceived exertion as an indicator of somatic stress. *Scand J Rehabil Med* 1970; **2:** 92–98.
15. Vanhees L, Kornaat M, Defoor J, Aufdemkampe G, Schepers D, Stevens A, et al. Effect of exercise training in patients with an implantable cardioverter defibrillator. *Eur Heart J* 2004; **25:** 1120–1126.
16. Fitchet A, Doherty PJ, Bundy C, Bell W, Fitzpatrick AP, Garratt CJ. Comprehensive cardiac rehabilitation programme for implantable cardioverter-defibrillator patients: A randomized controlled trial. *Heart* 2003; **89:** 155–160.
17. Berger R, Strecker K, Bojic A, Moser P, Stanek B, Pacher R. B-type natriuretic peptide predicts sudden death in patients with chronic heart failure. *Circulation* 2002; **105:** 2392–2397.
18. Davos C, Francis DP, Coats AJ; ExTraMATCH Collaborative. Exercise training meta-analysis of trials in patients with chronic heart failure (ExTraMATCH). *BMJ* 2004; **328:** 189–192.